IC/84/18

INTERNATIONAL CENTRE FOR THEORETICAL PHYSICS

INELASTIC ELECTRON SCATTERING FORM FACTORS INVOLVING THE SECOND EXCITED 2^+ LEVELS IN THE NUCLEI ^{48}Ti AND ^{50}Cr

G. Mukherjee

and

S.K. Sharma

INTERNATIONAL ATOMIC ENERGY AGENCY

UNITED NATIONS EDUCATIONAL, SCIENTIFIC AND CULTURAL ORGANIZATION

1984 MIRAMARE-TRIESTE

International Atomic Energy Agency

and

United Nations Educational Scientific and Cultural Organization

INTERNATIONAL CENTRE FOR THEORETICAL PHYSICS

INELASTIC ELECTRON SCATTERING FORM FACTORS INVOLVING THE SECOND EXCITED 2^+ LEVELS IN THE NUCLEI ^{48}Ti and ^{50}Cr *

G. Mukherjee

Department of Physics, Indian Institute of Technology Kanpur

Kanpur - 20 8016, India,

and

S.K. Sharma **

International Centre for Theoretical Physics, Trieste, Italy.

MIRAMARE - TRIESTE

March 1984

* To be submitted for publication.

** Permanent Address: Department of Physics, Indian Institute of Technology Kanpur, Kanpur - 20 8016, India.

ABSTRACT

A microscopic description of the recent data on the Coulomb form factors for the $0^+_{gnd} \rightarrow 2^+_2$ transitions in the nuclei ^{48}Ti and ^{50}Cr is attempted in terms of the prolate and oblate intrinsic states resulting from realistic effective interactions operating in the 2p - 1f shell. The results for the higher momentum-transfer region show dramatic improvements compared to the form factor estimates obtained in some recent shell model calculations involving the $f^n_{7/2} + f^{n-1}_{7/2} p_{3/2}$ configurations.

Inelastic electron scattering provides significant information concerning nuclear structure [1),2)]. Measurement of the cross section for the scattered electron permits one to determine the Fourier transform of the charge and nuclear-current densities for the nuclear states involved in the transition. In contrast with the experimental studies with ordinary γ transitions, the spatial structure of the nuclear matrix elements is expected to provide a sensitive test of the nuclear wave functions as well as the transition operators involved in the theoretical description.

Some recent inelastic electron scattering experiments [3)-5)] have provided valuable data on the $0^+_{gnd} \rightarrow 2^+_1$ as well as $0^+_{gnd} \rightarrow 2^+_2$ transitions in the N=26 nuclei ^{48}Ti and ^{50}Cr. Within a measured momentum-transfer range upto $q_{eff} \sim 2$ fm^{-1}, the C2 form factors involving $0^+_{gnd} \rightarrow 2^+_1$ transitions are characterized by two peaks appearing at $q_{eff} \sim 0.7$ fm^{-1} and $q_{eff} \sim 1.7$ fm^{-1}. Although the qualitative features of the form factors associated with $0^+_{gnd} \rightarrow 2^+_2$ transitions are quite similar to those of the observed form factors for the $0^+_{gnd} \rightarrow 2^+_1$ transitions, the magnitudes of $|F|^2$ for the former transitions are smaller by an order of magnitude than those for the latter.

Recently Iwamoto et al.[6)] studied the C2 form factors involving the first and the second excited 2^+ states in some Ti and Cr isotopes in terms of the wave functions resulting from empirical effective interactions operating in the restricted valence space consisting of the $f^n_{7/2} + f^{n-1}_{7/2} p_{3/2}$ configurations. In their work Iwamoto et al.[6)] employed the empirical effective interactions given by Oda et al.[7)] as well as by Yokoyama et al.[8)] The results for the low momentum-transfer ($q_{eff} < 1.5$ fm^{-1}) region of $|F|^2(0^+_{gnd} \rightarrow 2^+_1)$ were consistent with experiments; the results were also quite stable towards the choice of different effective interactions. However, the choice of the $f^n_{7/2} + f^{n-1}_{7/2} p_{3/2}$ space proved too restrictive to permit an unambiguous interpretation of the available data for the high momentum-transfer part of the $0^+_{gnd} \rightarrow 2^+_1$ transition, as well as the $0^+_{gnd} \rightarrow 2^+_2$ transition involving 0.5 fm$^{-1} < q_{eff} < 2.0$ fm^{-1} ; the calculated results displayed large variation with respect to the choice of the effective interactions. Furthermore,

none of the two effective interactions yielded acceptable simultaneous agreement for the $0^+_{gnd} \rightarrow 2^+_1$ as well as the $0^+_{gnd} \rightarrow 2^+_2$ transitions, although relatively large values of the neutron effective charges – $e_n = 1.0e$ and $e_n = 1.2e$ for the nuclei ^{48}Ti and ^{50}Cr, respectively – were employed.

We have recently shown [9] that the yrast wave functions projected from the Hartree-Fock-Bogolubov (HFB) intrinsic states of prolate shapes resulting from a slightly modified version of the Kuo-Brown (KB) effective interaction [10),11)] for the full 2p – 1f space provide a good description of the observed form factors for the $0^+_{gnd} \rightarrow 2^+_1$ transitions in several 2p – 1f shell nuclei. The purpose of this paper is to show that a fairly satisfactory interpretation of the available $|F|^2$ data for the $0^+_{gnd} \rightarrow 2^+_2$ transitions in the nuclei ^{48}Ti and ^{50}Cr can also be attempted in terms of reasonable values of the proton and neutron effective charges by describing the yrare states in terms of the oblate variational solutions resulting from the modified KB interaction.

The details concerning the calculation of the inelastic scattering form factors in terms of projected HFB wave functions have been discussed in our earlier work [9]. The intrinsic deformed HFB state with K=0 can be written, in the usual notation, as

$$|\Phi_o\rangle = \prod_{im} (u_i^m + v_i^m \; b_{im}^\dagger \; b_{i\bar{m}}^\dagger) \, |0\rangle \qquad (1)$$

where the creation operators $b_{im}^\dagger$ can be expressed as

$$b_{im}^\dagger = \sum_j c_{ji}^m \; a_{jm}^\dagger \; ; \; b_{i\bar{m}}^\dagger = \sum_j c_{ji}^m \; (-1)^{j-m} \; a_{j-m}^\dagger \qquad (2)$$

Here j labels the spherical single particle orbits ($1f_{7/2}$, $2p_{3/2}$, $2p_{1/2}$, $1f_{5/2}$).

The eigenstates of $\hat{J}^2$ projected from the HFB state $|\Phi_K(\delta)\rangle$ can be written as

$$|\Psi^J_K(\delta)\rangle = P^J_{KK} \, |\Phi_K\rangle = \frac{2J+1}{8\pi^2} \int D^J_{KK}(\Omega) \; R(\Omega) \; |\Phi_K\rangle \, d\Omega \qquad (3)$$

where $R(\Omega)$ and $D^J_{KK}(\Omega)$ are the rotation operator and the rotation matrix, respectively. Here δ denotes the quadrupole deformation of the intrinsic state.

Neglecting the transverse scattering of electrons the cross section is described by Coulomb scattering alone. In the framework of the plane wave Born approximation (PWBA) the squared form factor $|F|^2$ is given by [1), 2)]

$$|F(q)|^2 = \frac{4\pi}{Z^2} \; \frac{1}{(2J_i+1)} \; |\langle J_f(\delta_2) \| f^{(L)} \| J_i(\delta_1) \rangle|^2 \qquad (4)$$

where Z is the atomic number of the target nucleus. Here $J_i(\delta_1)$ and $J_f(\delta_2)$ denote the initial and the final scattering states resulting from angular momentum projection on the intrinsic states $|\Phi_K(\delta_1)\rangle$ and $|\Phi_K(\delta_2)\rangle$, respectively. The one-body operator $f^{(L)}_M$ is given by

$$f^{(L)}_M = \sum_k e_k \; j_L(qr_k) \; Y^{(L)}_M(\Omega_k) \qquad (5)$$

where e_k is the charge on the k-th nucleon, q is the momentum-transfer, j_L is the spherical Bessel function and $Y^{(L)}_M$ is the spherical harmonics of order L.

The centre-of-mass correction and the proton finite-size effect are taken into account by multiplying factors $\exp\left[b^2q^2/4\right]$ and $\exp\left[-a_p^2 \, q^2/4\right]$ respectively, where $a_p = 0.59$ fm and b (oscillator parameter) = $1.01 \; A^{1/3}$ fm.

Further, in order to compare the form factors calculated by PWBA with the experimental ones, the experimental data have been plotted at the effective momentum-transfer [12)] q_{eff} instead of the kinematic q:

$$q_{eff} = q \left[1 + \frac{3\sqrt{3}}{2\sqrt{5}} \; \frac{Ze^2}{R} \right] \qquad (6)$$

where R is the rms radius and E is the energy of the incident electrons.

In our calculations we have employed the Kuo-Brown effective interaction [10)] for the ($1f_{7/2}$, $2p_{3/2}$, $2p_{1/2}$, $1f_{5/2}$)^n space, slightly

modified by Mc Grory et al.[11] so as to optimize the agreement between the shell model and the experimental spectra for some Ca isotopes. The single-particle energies are taken from the ^{41}Ca spectrum. This set of input parameters is the same as the one employed in our earlier calculation[9] of inelastic electron scattering form factors for the excitation of 2^+_1 state in some 2p-1f shell nuclei.

Table I summarizes our results concerning the self-consistent intrinsic states associated with the yrast as well as the yrare bands in the nuclei ^{48}Ti and ^{50}Cr. It can easily be seen that the calculated energy separation between the prolate and oblate variational solutions in these nuclei are consistent with the observed excitation energies of the 2^+_2 states relative to the 0^+_{gnd} states. The difference in the intrinsic energies of the prolate and oblate solutions represents roughly the difference in the energies of the $J^\pi = 0^+$ states projected from these solutions. Further, the excitation energies of the 2^+_2 states relative to the 0^+_2 states are usually about 1 MeV in the nuclei with N=26 in the 2p-1f shell; this assumption is supported by earlier calculations[13] involving explicit angular momentum projection on the intrinsic states with quadrupole deformations quite similar to the ones calculated here, as well as by the observed $[E(2^+_2) - E(0^+_2)]$ differences in the nuclei ^{48}Ti and ^{50}Cr. Thus, the results given in Table I imply that the $J^\pi = 2^+_2$ states projected from the oblate intrinsic wave function in the nuclei ^{48}Ti and ^{50}Cr are likely to occur at 2.3 MeV and 2.8 MeV, respectively, relative to the ground states. These estimates are remarkably close to the observed excitation energies of the 2^+_2 states — 2.42 MeV and 2.92 MeV— in the nuclei ^{48}Ti and ^{50}Cr respectively. It is thus reasonable to expect that an adequate description of the observed 0^+_{gnd} and 2^+_2 states can be obtained by projecting them from the prolate and oblate intrinsic wave functions, respectively.

Fig. 1 compares the calculated and experimental $|F|^2$ for the $0^+_{gnd} \longrightarrow 2^+_1$ as well as $0^+_{gnd} \longrightarrow 2^+_2$ transitions in the nucleus ^{48}Ti. We have also given here the results obtained by Iwamoto et al.[6] in the framework of the shell model involving the $f^n_{7/2} + f^{n-1}_{7/2}\, p_{3/2}$ configurations.

In the earlier work two sets of empirical effective interactions were employed. One was the set of matrix element obtained by Oda et al.[7] through a chi-square fit to the 38 levels chosen from Ca and Sc isotopes and the other was the set obtained by Yokoyama et al.[8] through a fit to the 63 data selected from the N=27 and 28 isotones (A= 47-55). Hereafter we shall refer to these sets of matrix elements as the V(Ca -Sc) and the V(27-28) interactions, respectively.

The results presented in Fig. 1 bring out the sensitivity of the restricted shell model calculations for the high momentum-transfer part of the form factors associated with the $0^+_{gnd} \longrightarrow 2^+_{1,2}$ transitions towards the choice of the effective interactions. Further, none of the effective interactions employed earlier in conjunction with the $f^n_{7/2} + f^{n-1}_{7/2}\, p_{3/2}$ space provides an adequate simultaneous interpretation of the available data involving both the $0^+_{gnd} \longrightarrow 2^+_1$ as well as the $0^+_{gnd} \longrightarrow 2^+_2$ transitions. Whereas the interaction V(Ca - Sc) leads to reasonable agreement with the experiments for $q_{eff} > 1.5$ fm^{-1} in the case of the $0^+_{gnd} \longrightarrow 2^+_1$ transition, the calculated values (not shown in the figure) for high momentum-transfer involving the $0^+_{gnd} \longrightarrow 2^+_2$ transition are smaller by more than an order of magnitude. The shell model estimates for $|F|^2$ around its second maximum obtained with the interaction V(27 - 28), on the other hand, are smaller than the observed ones by roughly a factor of two for the $0^+_{gnd} \longrightarrow 2^+_1$ as well as the $0^+_{gnd} \longrightarrow 2^+_2$ transitions.

It is seen that the present calculation yields an adequate overall quantitative description of the available data for both the $0^+_{gnd} \longrightarrow 2^+_1$ as well as the $0^+_{gnd} \longrightarrow 2^+_2$ transitions. In particular, the PHFB values for the squared form factor around $q_{eff} = 1.7$ fm^{-1} show substantial improvements over the earlier results. Our choice of the neutron effective charge also contrasts keenly with the values employed in the earlier work. The present calculation involves the effective charges $(e_p, e_n) = (1.4\ e,\ 0.4\ e)$ whereas the restricted shell model calculation employed $(e_p, e_n) = (1.4\ e, 1.0\ e)$.

A significant discrepancy between the calculated and the observed results occurs around the first maximum associated with the $0^+_{gnd} \longrightarrow 2^+_2$ transition where the PHFB results overestimate the observed values by about

a factor of two. In view of the sensitivity of the form factors for the $0^+_{gnd} \longrightarrow 2^+_2$ transition towards small configurational admixtures, an inclusion of the quasiparticle excitations in the oblate HFB states is likely to result in further improvements.

We next discuss the results for the nucleus ^{50}Cr. We have employed the same set of effective charges — $e_p = 1.4$ e and $e_n = 0.4$ e — as the ones employed in the nucleus ^{48}Ti. The effective charges employed in the earlier shell model calculation, however, are $(e_p, e_n) = (1.6\,e, 1.2\,e)$. In view of the relatively large values of the calculated intrinsic quadrupole moments for the yrast states (see column 4, Table I), one expects an enhanced involvement of the configurations outside the $(f^n_{7/2} + f^{n-1}_{7/2}\, p_{3/2})$ space in the nucleus ^{50}Cr. The increased values of the effective charges employed in the earlier work [6] are intended to simulate this effect to some extent.

In the nucleus ^{48}Ti only the part of the calculated form factor for the $0^+_{gnd} \longrightarrow 2^+_2$ transition involving $q_{eff} > 1.5$ fm^{-1} is found to be sensitive towards the choice of the effective interaction employed in the restricted shell model work. In contrast to this, even the low momentum-transfer part of the restricted shell model estimates for $|F|^2(0^+_{gnd} \longrightarrow 2^+_2)$ displays significant interaction dependence in the nucleus ^{50}Cr; the $|F|^2$ values resulting from V(Ca-Sc) and V(27-28) differ by more than a factor of 5 throughout the range $0.5\ \text{fm}^{-1} \lesssim q_{eff} \lesssim 2.0\ \text{fm}^{-1}$. Further, both the interaction V(Ca-Sc) as well as V(27-28) fail to reproduce even qualitatively the observed form factors for the $0^+_{gnd} \longrightarrow 2^+_2$ transition; the magnitude of $|F|^2$ around its second minimum are much too low compared with the experiments.

The use of the projected HFB wave functions for the 2^+_2 state leads to the required enhancement around the second maximum. One also observes a shift of the dip in the $|F|^2$ values towards the lower momentum-transfer region. Although the PHFB results for the $0^+_{gnd} \longrightarrow 2^+_2$ form factors for $q_{eff} \sim 0.8$ fm^{-1} are still somewhat larger compared to the experiments, the present calculation is seen to yield significant improvement vis-á-vis simultaneous description of the form factors for the $0^+_{gnd} \longrightarrow 2^+_1$

as well as the $0^+_{gnd} \longrightarrow 2^+_2$ transitions in the nucleus ^{50}Cr.

As mentioned earlier, an important feature that characterizes the observed form factors for the $0^+_{gnd} \longrightarrow 2^+_2$ transitions in the nuclei ^{48}Ti and ^{50}Cr is their reduced magnitude — by an order of magnitude — compared to those for the $0^+_{gnd} \longrightarrow 2^+_1$ transitions. Present microscopic description offers a qualitative understanding of this feature of the $0^+_{gnd} \longrightarrow 2^+_2$ transitions in terms of the reduced overlap between the initial (0^+_{gnd}) and the final (2^+_2) states due to their different intrinsic parentage.

Summarizing, we have shown that the use of the yrast and yrare states with $J^\pi = 0^+, 2^+$ projected from self-consistent prolate and oblate intrinsic states resulting from the modified KB interaction for the 2p-1f shell permits a reasonably adequate simultaneous description of the observed data involving the $0^+_{gnd} \longrightarrow 2^+_1$ as well as $0^+_{gnd} \longrightarrow 2^+_2$ transitions in the nuclei ^{48}Ti and ^{50}Cr.

ACKNOWLEDGMENTS

One of the author (S.K.S.) would like to thank Professor Abdus Salam and Professor L. Fonda, as well as the International Atomic Energy Agency and UNESCO for hospitality at the International Centre for Theoretical Physics, Trieste.

REFERENCES

1) T. de Forest and J. Walecka, Adv.Phys. 15, 1 (1966).

2) H. Überall, Electron Scattering From Complex Nuclei (Academic, New York 1971).

3) A. Hotta et al., Res. Rep. Nucl.Sc. (Tohoku University) 9, 7 (1976); 10, 18 (1977).

4) K. Hosoyama et al., Res.Rep.Nucl.Sc. (Tohoku University) 11, 1 (1978).

5) J.W. Lightbody Jr. et al., Bull.Am.Phys.Soc. 20, 568 (1975).

6) T. Iwamoto, H. Horie and A. Yokoyama, Phys.Rev. C25, 658 (1982).

7) T. Oda, K. Muto and H. Horie, Lett. Nuovo Cimento 18, 549 (1977).

8) A. Yokoyama, T. Oda and H. Horie, Prog.Theor.Phys. 60, 427 (1978).

9) G. Mukherjee and S.K. Sharma, Phys.Rev. C (in press).

10) T.T.S. Kuo and G.E. Brown, Nucl.Phys. A114, 241 (1968).

11) J.B. Mc Grory, B.H. Wildenthal and E.C. Halbert, Phys.Rev. C2, 182 (1970).

12) A. Bohr and B.R. Mottelson; Nuclear Structure, (Benjamin, New York-Amsterdam 1969) Vol.I, P. 145.

13) S.K. Sharma, Nucl.Phys. A260, 226 (1976).

TABLE I

Details of the variational intrinsic states associated with the yrast as well as the yrare levels in the nuclei ^{48}Ti and ^{50}Cr. The intrinsic quadrupole moments have been given in units of b^2, where $b=(\hbar/M\omega)^{1/2}$. Here $\langle Q_0^2\rangle_\pi$ ($\langle Q_0^2\rangle_\nu$) gives the contribution of protons (neutrons) towards the total quadrupole moment.

Nucleus	Variational Solution	E(MeV)	$\langle Q_0^2\rangle\left[\langle Q_0^2\rangle_\pi, \langle Q_0^2\rangle_\nu\right]$
^{48}Ti	Prolate	- 17.5	16.7 [6.8, 9.9]
	Oblate	- 16.2	-13.7 [-6.0,-7.7]
^{50}Cr	Prolate	- 29.9	25.5 [12.7, 12.8]
	Oblate	- 28.1	-12.7 [-6.5, -6.2]

FIGURE CAPTIONS

Fig. 1 : Experimental [3),4)] and calculated squared form factors $|F|^2$ for the $0^+_{gnd} \longrightarrow 2^+_{1,2}$ transitions in the nucleus ^{48}Ti. The broken and the dotted-dashed curves represent the results obatined by Iwamoto et al.[6)] with the empirical effective interactions V(27-28) and V(Ca-Sc), respectively, in conjuction with the $f^n_{7/2} + f^{n-1}_{7/2}\, p_{3/2}$ configurations. The solid curves give the results obtained in the present calculation.

Fig. 2 : Experimental [5)] and calculated squared form factors $|F|^2$ for the $0^+_{gnd} \longrightarrow 2^+_{1,2}$ transitions in the nucleus ^{50}Cr.

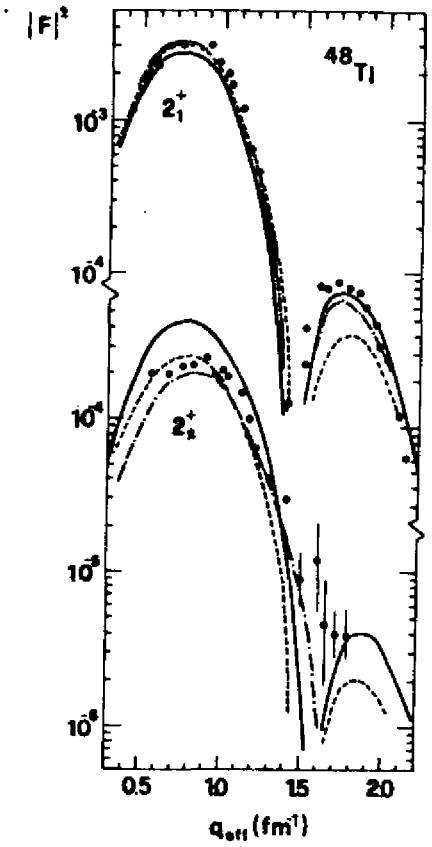

Fig.1

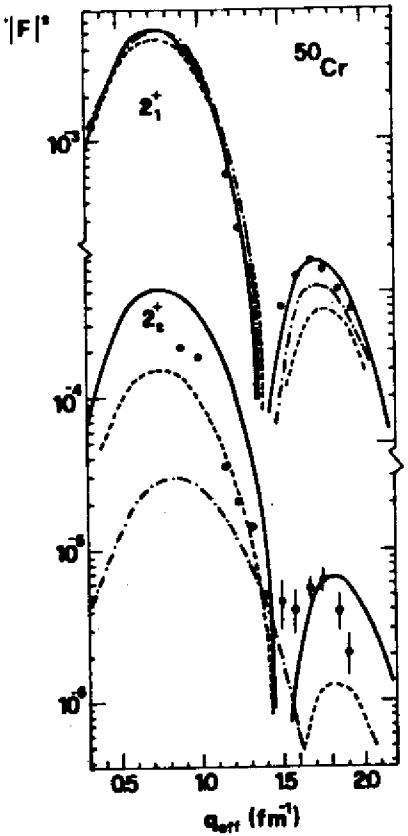

Fig.2